Pre-themalizational effect of hot carriers on photovoltage formation in a solar cell

Masalskyi O. and Gradauskas J.

Vilnius Gediminas Technical University, Saulėtekio Avenue 11, 10223 Vilnius, Lithuania vilniustech@vilniustech.lt

Received: 14.03.2022

Abstract. Although the power-conversion efficiency of single-junction solar cells achieved in practice is slowly increasing in the recent years, it still remains well below the theoretical Shockley–Queisser limit. We analyze in this relation the impact of hot carriers which represents an additional fundamental mechanism of intrinsic losses. We suggest that it is one of the reasons why the theoretical efficiency limit cannot be reached. We demonstrate that all of the solar photons participate in carrier heating, except for those having the energy equal to the bandgap. This supplies the process with more than 52% of the total incident solar energy. Finally, we give experimental evidence to a hot-carrier photovoltage (PV) arising in Si and GaAs cells before thermalization process. This PV is opposite to a classical PV induced by carrier generation, thus hindering the efficiency of p-n-junction solar cells.

Keywords: solar cells, p-n junctions, photovoltage, hot carriers, efficiency

UDC: 535.215

1. Introduction

A first glance at practical power-conversion efficiencies reported by the National Renewable Energy Laboratory since 1977 [1] gives an impression that the efficiency evolution of a classical single-crystal silicon solar cells has reached its saturation. Marked efficiency improvements have mainly been achieved due to engineering, technological or cell-design novelties like PERC (Passivated Emitter and Rear Cell) and PERL (Passivated Emitter and Rear Locally-Diffused) structures in 1990s, or due to introduction of silicon heterojunctions later on [2]. The record level of 26.1% at one sun illumination is still far below the theoretical Shockley–Queisser limit of about 32% [3].

In general, all the loss processes that hinder reaching the limit can be divided into two categories. The extrinsic losses result from series resistance, unacceptable recombination and grid shadowing. All of these are not taken into account when calculating the limiting efficiency so that they can be minimized or even avoided owing to technological or design-related measures. As a rule, the unavoidable fundamental intrinsic-loss processes in single-bandgap (E_g) solar cells are classified as follows [4]: (1) a below-E_g loss (photons with the energy lower than the bandgap are supposed to be not absorbed at all), (2) a thermalization loss (a high photon energy left over generation is dissipated in crystal lattice), (3) an emission loss, (4) a Carnot loss, and (5) a Boltzmann loss. The first two mechanisms dominate and amount up to 57.9% or 60.0% of total intrinsic losses in silicon or GaAs solar cells, respectively (see Table 1).

In the present work we consider a hot-carrier effect as an additional fundamental intrinsic-loss mechanism. In photovoltaics, hot carriers attract attention mostly in connection with the development of hot-carrier solar cells which have potentially a 66% maximum efficiency [5]. In

Table 1. Below-bandgap and thermalization losses occurring in Si and GaAs solar cells [4], and the corresponding contributions of incident solar spectrum into electron–hole pair generation and carrier heating, according to Fig. 1.

Loss process, %	Si	GaAs	Source
Below-E_g	17.2	33.8	[4]
Thermalization	40.7	26.2	[4]
Solar-spectrum contribution, %			
Generation	47.8	45.3	this work
Hot carriers ($h\nu < E_g$)	19.0	33.0	this work
Hot carriers ($h\nu > E_g$)	33.2	21.7	this work

spite of numerous efforts to create acceptable absorbers [6–8] and energy-selective contacts [9–11], which are necessary to harness the excess energy of light-heated carriers, only a few studies on the practical realization of hot-carrier solar cells have been reported up to now [12, 13]. The main drawback to this progress is very fast dissipation of hot-carrier energy occurring in a crystal lattice (i.e., a thermalization processes lasting within a picosecond range) [14]. In spite of a very short time of 'hot state', a clear possibility to employ hot carriers in photovoltaics has already been demonstrated. For example, a hot-carrier photovoltage (HCPV) has been induced across l-h semiconductor junctions under the action of laser pulses with the photon energy $h\nu < E_g$ [15, 16]. Being exposed to CO_2-laser light ($h\nu = 0.12$ eV), Ge, Si and GaAs p-n junctions have also demonstrated an increase in the HCPV [17–19]. It is worthwhile that the polarity of HCPV indicates a diffusion of light-heated carriers up the potential barrier of a junction, in contrast to a classical photovoltage (PV) resulting from electron–hole pair generation. Moreover, both two-photon absorption-caused generation and HCPV have been simultaneously detected across a p-n junction in case of the photon energies $h\nu < E_g < 2h\nu$ [20, 21]. The polarities of these PVs are opposed to each other.

In this work we continue to study the impact of hot carriers on the PV formed across a single-junction solar cell. Both theoretical considerations and experimental proof of the hot-carrier effect are presented. To investigate the effect, we have chosen silicon and gallium arsenide semiconductors having distinct properties. Being the most widely used photovoltaic material, Si has an indirect bandgap and weaker interband optical absorption. On the other hand, GaAs represents a direct-bandgap semiconductor and its bandgap, $E_g = 1.42$ eV, is very close to the optimal theoretical value of 1.4 eV corresponding to the maximal possible efficiency in single-junction solar cells [22].

2. Results and discussion

Our spectral studies are based on a simple assumption that a part of solar radiation,

$$I_G = I_0 \frac{E_g}{h\nu}, \tag{1}$$

generates electron–hole pairs for all the photons with the energies $h\nu \geq E_g$, whereas the rest of solar energy,

$$I_{hc} = \begin{cases} I_0 \dfrac{h\nu - E_g}{h\nu}, & \text{for} \quad h\nu > E_g \\ I_0, & \text{for} \quad h\nu < E_g \end{cases}, \tag{2}$$

goes to free-carrier heating. In Eqs. (1) and (2), I_0 stands for the incident solar radiation.

Fig. 1 shows the spectral distributions calculated with Eqs. (1) and (2) for the cases of Si and GaAs. As for silicon, the calculations reveal that 19.0% and 33.2% of the total AM 1.5 G solar radiation can heat carriers with the low-energy ($h\nu < E_g$) and high-energy ($h\nu > E_g$) photons, respectively. The figures 33.0% and 21.7% can be obtained in the case of gallium arsenide. As seen from Table 1, a quite good percentage agreement is achieved between the case of low-energy photons with the below-bandgap loss. A bigger discrepancy between the hot-carrier contribution and the thermalization loss appears in the short-wavelength range. Most probably, it is due to different light sources adopted: the authors of Ref. [4] have modelled the Sun as a blackbody (with the temperature $T = 6000$ K), while we use the solar spectrum for the terrestrial air mass 1.5. Nevertheless, the both approaches agree with each other in the fact that more than a half of the incident solar radiation takes part in the heating of carriers.

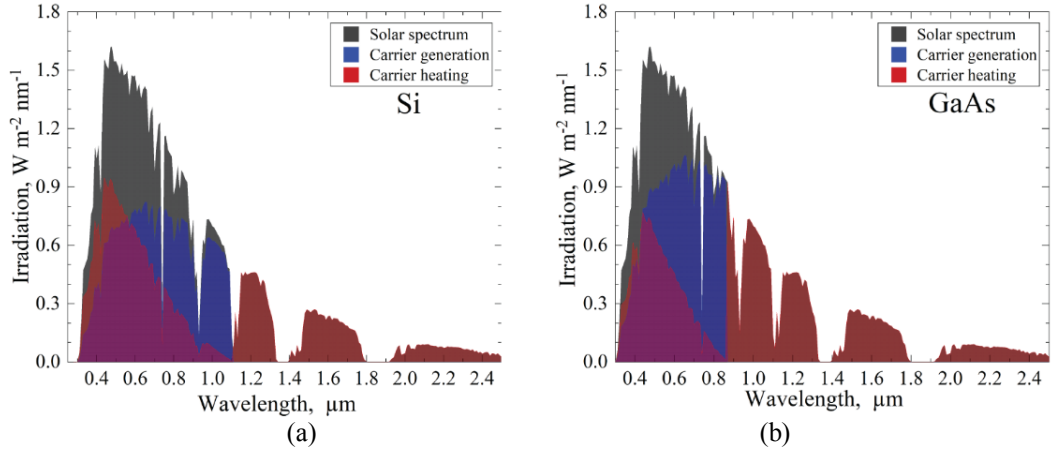

Fig. 1. A terrestrial air mass 1.5 solar spectrum (grey), and its contributions into carrier generation (blue) and potential carrier heating (red) in silicon (a) and GaAs (b).

A somewhat different pattern appears when the effect of light absorption in semiconductors is taken into account in the solar spectral range. The absorbed solar irradiance reads as

$$I_{abs} = 1 - I_0 e^{-\alpha x}, \tag{3}$$

where α stands for the absorption coefficient and x for the depth of light penetration. The data for α has been taken from Refs. [23–25]. To find the appropriate generation and hot-carrier parts of the absorbed radiation, we substitute I_0 with I_{abs} in Eqs. (1) and (2). Fig. 2 depicts the spectral distributions of the absorbed radiation and its parts associated with carrier generation and heating in a semiconducting sample with the carrier density $n = 10^{19}$ cm^{-3} and the thickness $x = 500$ nm. The corresponding data is given in Table 2.

As the calculations show, the portion of total absorbed solar radiation spent for carrier heating in silicon even exceeds that spent for carrier generation and a consequent functional electric-power generation. Of course, the most of the absorbed solar energy which contributes to carrier heating comes from the interband absorption when the photon energy is given by $h\nu > E_g$, since the absorption by free carriers (i.e., the intraband one corresponding to the case of $h\nu < E_g$) is an order of magnitude weaker within the solar spectrum [23]. In GaAs, the contribution of carrier generation prevails over that of carrier heating (see Table 2), since the bandgap of this semiconductor better fits the solar spectrum in the sense of optimal value of the maximal possible efficiency. In any case, the intraband absorption is also noteworthy and its impact has to be taken into account.

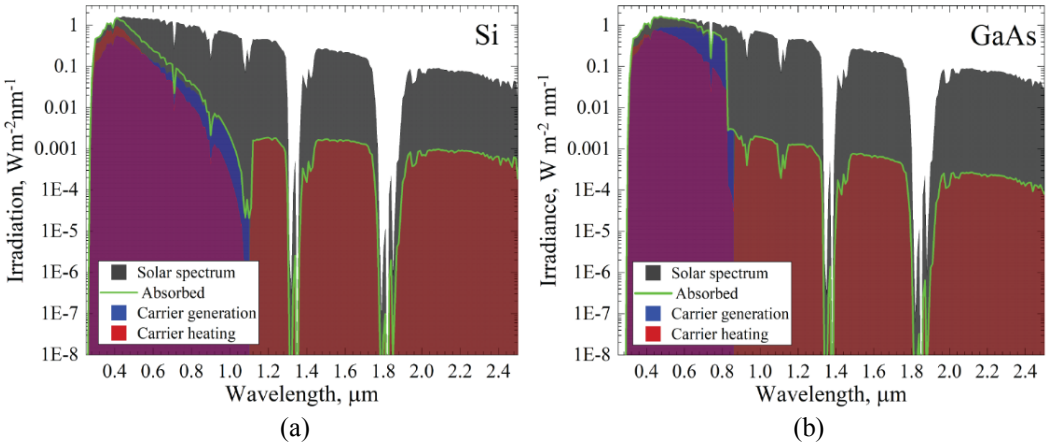

Fig. 2. A terrestrial air mass 1.5 solar spectrum (grey), its absorbed part (green) and a portion of the absorbed part spent at carrier generation (blue) and potential carrier heating (red) in silicon (a) and GaAs (b), as calculated using Eq. (3). The carrier density is equal to $n = 10^{19}$ cm^{-3} and the light-penetration depth to $x = 500$ nm.

Table 2. Contributions of solar spectrum absorbed by silicon and gallium arsenide, as calculated according to Eq. (3). The carrier density is equal to $n = 10^{19}$ cm^{-3} and the light-penetration depth to $x = 500$ nm.

Absorbed solar-spectrum contribution, %	**Si**	**GaAs**
Generation	40.2	63.5
Hot carriers ($h\nu < E_g$)	0.5	0.2
Hot carriers ($h\nu > E_g$)	59.3	36.3

Fig. 3 presents dependences of the parts of absorbed solar radiation within the spectral range $h\nu < E_g$ on the carrier density, as calculated at different light penetration depth ($x = 100$–5000 nm). A nearly linear increase (see a dashed line in Fig. 3), especially that occurring at higher density values, is a characteristic feature of the process of intraband free-carrier absorption. In the case of typical silicon-based solar cells with an 0.5 μm-thick emitter doped up to $n = 10^{20}$ cm^{-3}, the part of the absorbed solar radiation in the infrared region ($h\nu < E_g$) can exceed 4%. This amount of the absorbed radiation also contributes to the carrier heating, thus hindering efficient operation of a solar cell.

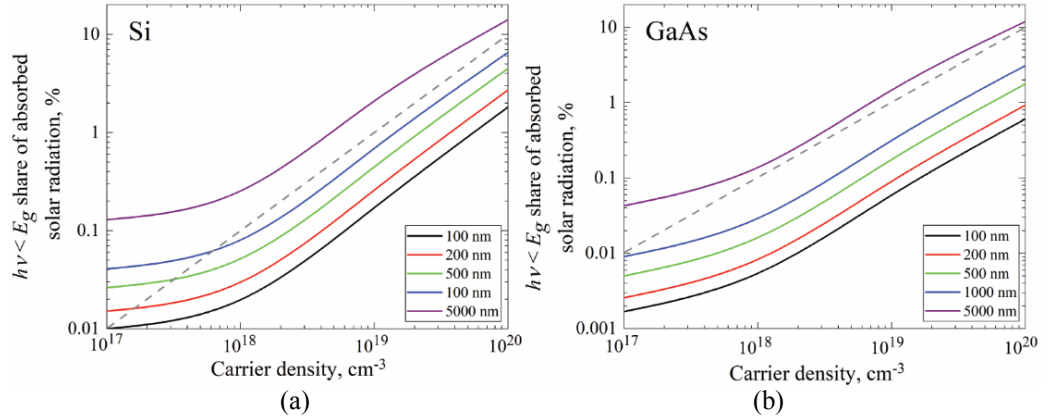

Fig. 3. Dependences of the parts of absorbed solar radiation in the spectral range $h\nu < E_g$ on the carrier density, as obtained at different light-penetration depths x (from 100 to 5000 nm). Panels (a) and (b) correspond respectively to Si and GaAs. Dashed lines are guides for eye of a linear dependence.

Hence, the above theoretical evaluations of possible carrier heating within the solar spectrum encourage experimental studies of the HCPV effect in solar cells. We prepared p-n-junction-containing Si samples from industrial silicon solar cells (SoliTek, Vilnius, Lithuania). The carrier densities in emitter and base were $n \sim 10^{20}$ cm^{-3} and $p = 10^{16}$ cm^{-3}, respectively. Samples of gallium arsenide were liquid-phase epitaxy-grown, with the carrier densities $p = 5\times10^{17}$ cm^{-3} of top emitter and $n = 3\times10^{17}$ cm^{-3} of bottom base. They were doped respectively with Zn and Te. More details about GaAs-sample preparation had been reported elsewhere (see Ref. [26]).

The samples cut to the dimensions 2×2 mm^2 were exposed to radiation of two different lasers. One laser had the wavelength 1.06 μm, the pulse duration 25 ns, the repetition rate 50 Hz and the maximum intensity 10 MW/cm^2. The appropriate parameters of the other laser were 1.34 μm, 1.7 ns, 50 Hz and 0.4 MW/cm^2. Short laser pulses were preferable to enable detecting fast hot-carrier effects, as compared to much slower carrier-recombination processes. All the experiments were carried out at the room temperature.

Fig. 4 shows transients of the PV pulses taking place across the p-n junctions exposed to the laser radiation with the photon energy $h\nu = 0.92$ eV (the corresponding wavelength 1.34 μm). As seen from Fig. 4a, the photoresponse of silicon cell ($E_g = 1.12$ eV) consists of two sub-pulses having the opposite polarities. Since the photon energy is less than (though not so far from) the fundamental absorption edge, the PV of positive polarity can be undoubtedly attributed to the generation of carriers and their separation inside the p-n junction. A long-lasting relaxation of this component is defined by the carrier lifetime. The negative sub-pulse points to carrier flow in the opposite direction, i.e. up the potential barrier of the junction. Its polarity and fast response speed are inherent features of the HCPV effect.

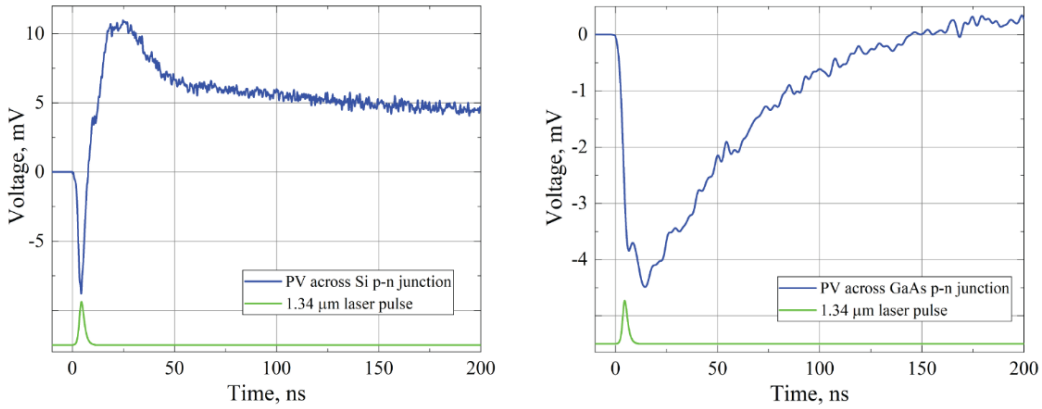

Fig. 4. PV induced by a 1.34-μm laser pulse (blue lines) across silicon (a) and GaAs (b) p-n junctions. No bias is applied and the laser intensity is $I = 0.4$ MW/cm^2. A negative component stands for HCPV and a positive one corresponds to electron–hole pair generation. Laser-pulse profiles with arbitrary vertical scale (green lines) are added as a guide to eye.

A different situation takes place when a wider-bandgap ($E_g = 1.42$ eV) GaAs semiconductor is irradiated (see Fig. 4b). Then the PV mainly includes a sub-pulse with the negative polarity. Contrary to the case of Fig. 4a, the latter lasts much longer than the laser pulse itself. This difference can be explained as follows. The free carriers absorb the radiation, become 'hot' and stay so during the whole time of excitation. They cause increase in the HCPV. When the laser pulse ends, the hot carriers release their energy to the lattice (a thermalization process), the p-n junction becomes heated, and a thermovoltage is induced across it. This signal lasts until the

junction reaches its equilibrium temperature. Note that the process of heat dissipation by the lattice is much longer than the energy dissipation by the hot carriers and, as a rule, it is characterized by the time constants of microseconds or even longer [27]. Finally, a weak long-lasting positive sub-pulse, most probably, results from a laser photon-activated thermal generation of electron–hole pairs occurring in GaAs.

As seen from Fig. 5a, no negative PV-signal component is detected when the single-junction solar cell based on Si is exposed to 1.06-μm laser radiation. In this case the photon energy is greater than the bandgap (1.17 eV versus 1.12 eV, respectively) and the interband absorption prevails over a much weaker free-carrier absorption [23]. However, a forward-bias voltage should favour a flow of hot carriers up the barrier, since it lowers the potential barrier of the p-n junction. Indeed, application of the forward bias highlights availability of the HCPV and reduces the contribution of generation-caused PV into the total photoresponse signal (see Fig. 5b).

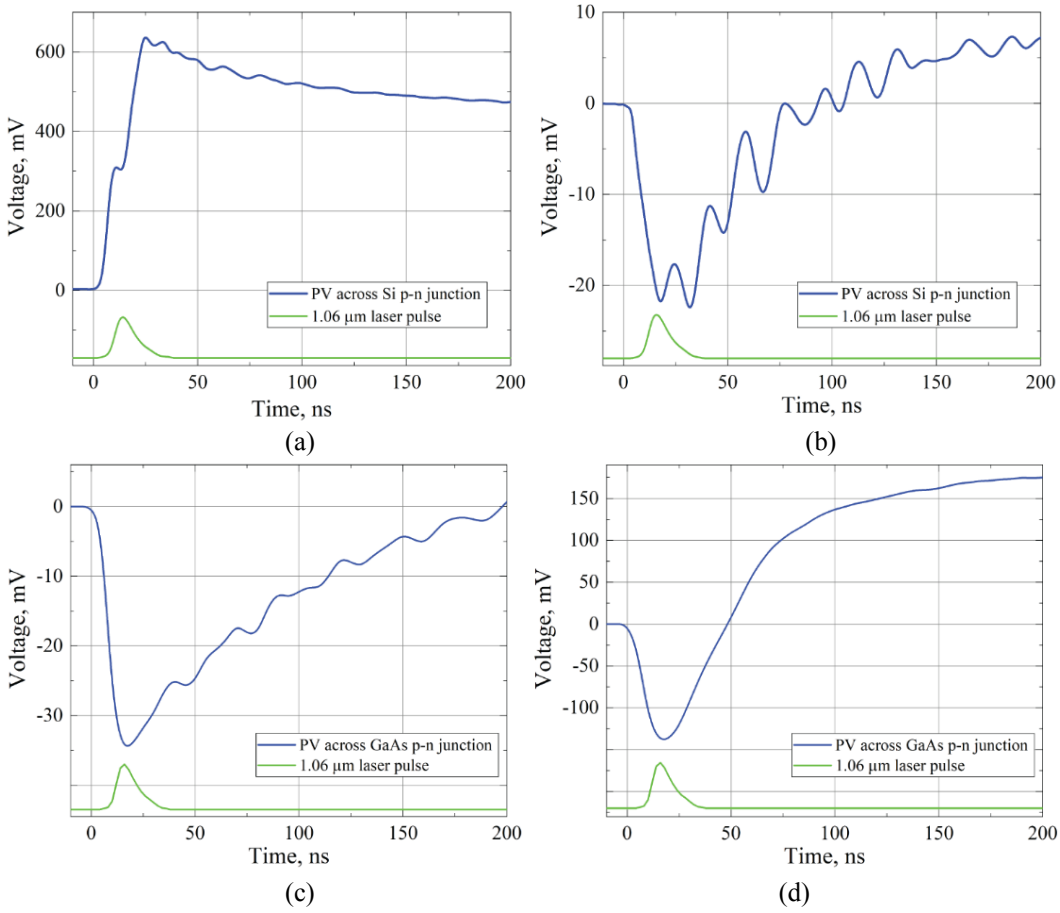

Fig. 5. PV induced by a 1.06-μm laser pulse (blue lines) across silicon (a, b) and GaAs (c, d) p-n junctions: (a) no bias and I = 0.4 MW/cm^2, (b) forward bias +0.85 V and I = 0.4 MW/cm^2, (c) no bias and I = 0.4 MW/cm^2, and (d) no bias and I = 4.2 MW/cm^2. A negative component stands for HCPV and a positive one corresponds to electron–hole pair generation. Laser-pulse profiles with arbitrary vertical scale (green lines) are added as a guide to eye.

Similar to the case of 1.34-μm laser irradiation, the GaAs p-n junction demonstrates increase in the HCPV occurring under the action of 1.06-μm laser pulses, since its E_g is still much more than the photon energy. It is worth noting that the HCPV dominates at low laser intensities (see Fig. 5c), although at higher intensities the generation-caused component develops as a result of two-photon absorption in GaAs sample [21].

3. Conclusion

Modelling of the absorption spectra of solar radiation in semiconductors reveals that both below- and above-bandgap solar photons have a potential to heat free charge carriers. Even small (though nonzero) contribution of the photons with the energies $h\nu < E_g$ into carrier heating can become pronounced in thick and heavily doped solar cells. Before thermalization processes and dissipation of their energy at crystal lattice, hot carriers can produce the effect of HCPV. We have testified the existence of this effect experimentally. It arises irrespective of solar photon-energy value in terms of the bandgap. Having the opposite polarity to that of the PV induced by carrier generation, the HCPV hinders efficient operation of the solar cells built upon p-n junctions. Hence, minimization of the HCPV effect can increase the efficiency of single-junction solar cells. On the other hand, it must be understood that the theoretical cell-efficiency limit would become lower if a direct negative impact of hot carriers were taken into account in the Shockley–Queisser theory. Namely, this limit would come closer to the solar-cell efficiency values achieved in practice recently.

Acknowledgement

This work was supported by the Research Council of Lithuania under the Grant № 01.2.2-LMT-K-718-01-0050.

References

1. The National Renewable Energy Laboratory (n. d.). Best Research-Cell Efficiency Chart. Nrel. Gov. Retrieved March 11, 2022. URL: https://www.nrel.gov/pv/cell-efficiency.html
2. Green M A, 2015. Forty years of photovoltaic research at UNSW. Journal and Proceedings of the Royal Society of New South Wales. **148**: 2–14.
3. Shockley W and Queisser H J, 1961. Detailed balance limit of efficiency of p-n junction solar cells. J. Appl. Phys. **32**: 510–519.
4. Hirst L C and Ekins-Daukes N J, 2011. Fundamental losses in solar cells. Prog. Photovolt. Res. Appl. **19**: 286–293.
5. Nozik A J, 2018. Utilizing hot electrons. Nature Energy. **3**: 170–171.
6. Shrestha S, Chung S, Liao Yu, Cao W, Gupta N, Zhang Y, Wen X, Conibeer G, 2017. Development of absorber and energy selective contacts for hot carrier solar cells. 2017 IEEE 44th Photovoltaic Specialist Conference (PVSC), pp. 696-700.
7. Dixit R, Barut B, Yin S, Nathawat J, Randle M, Arabchigavkani N, Kwan K He C-P, Mishima T D, Santos M B, Ferry D K, Sellers I R, and Bird J P, 2020. Pulsed studies of intervalley transfer in $Al_{0.35}In_{0.65}As$: a paradigm for valley photovoltaics. Phys. Rev. Mater. **4**: 1–8.
8. Frydendahl C, Grajower M and Bar-David J, 2020. Giant enhancement of silicon plasmonic shortwave infrared photodetection using nanoscale self-organized metallic films. Optica. **7**: 371–379.
9. Konovalov I and Ploss B, 2019. Modeling of hot carrier solar cell with semi-infinite energy filtering. Sol. Energy. **185**: 59–63.
10. Shayan S, Matloub S and Rostami A, 2018. Efficiency enhancement in a single bandgap silicon solar cell considering hot-carrier extraction using selective energy contacts. Opt. Express. **29**: 5068–5080.
11. Esgandari M, Barzinjy A A, Rostami A, Rostami G and Dolatyari M, 2022. Solar cells efficiency enhancement using multilevel selective energy contacts (SECs). Opt. Quantum Electron. **54**: 1–9.
12. Harada Y, Iwata N, Watanabe D, Asahi Sh and Kita T, 2019. Hot-carrier extraction in InAs/GaAs quantum dot superlattice solar cells. Hot-carrier extraction in InAs/GaAs quantum dot superlattice solar cells. IEEE 46th Photovoltaic Specialists Conference (PVSC), 2019, pp. 3004-3006.
13. Nguyen D-T, Lombez L, Gibelli F, Boyer-Richard S, Le Corre A, Durand O and Guillemoles J-F,

2018. Quantitative experimental assessment of hot carrier-enhanced solar cells at room temperature. Nature Energy. **3**: 236–242.
14. Liu Ch, Lu Y, Shen R, Dai Y, Yu X, Liu K and Lin Sh, 2022. Dynamics and physical process of hot carriers in optoelectronic devices. Nature Energy. **95**: 1–25.
15. Ašmontas S, Maldutis E and Širmulis E, 1988. CO_2 Laser radiation detection by carrier heating in inhomogeneous semiconductors. Int. J. Optoelectron. **3**: 263–266.
16. Ašmontas S., Gradauskas J., Seliuta D. and Širmulis E. 1999. Photoresponse in nonuniform semiconductor junctions under infrared laser excitation. Proc. SPIE 3890, Fourth International Conference on Material Science and Material Properties for Infrared Optoelectronics, (4 November 1999); **3890**:125-131.
17. Umeno M, Sugito Y, Jimbo T, Hattori H and Amenixa Y, 1978. Hot photo-carrier and hot electron effects in p-n junctions. Sol. State Electron. **21**: 191–195.
18. Encinas-Sanz F and Guerra J M, 2003. Laser-induced hot carrier photovoltaic effects in semiconductor junctions. Prog. Quant. Electron. **27**: 267–294.
19. Ašmontas S, Gradauskas J, Seliuta D and Širmulis E, 2000. Photoelectrical properties of nonuniform semiconductor under infrared laser radiation. Nonresonant Laser-Matter Interaction (NLMI-10), (26 June 2001). **4423**: 18-27.
20. Ašmontas S, Gradauskas J, Seliuta D, Sužiedelis A, Širmulis E, Valušis G and Tetyorkin V V, 2002. CO_2 laser induced hot carrier photoeffect in HgCdTe. Materials Science Forum. **384-385**: 147-150.
21. Ašmontas S, Gradauskas J, Sužiedelis A, Šilenas A, Širmulis E, Švedas V, Vaicikauskas V and Žalys O, 2018. Hot carrier impact on photovoltage formation in solar cells. Appl. Phys. Lett. **113**: 071103–071106.
22. Sven R, 2016. Tabulated values of the Shockley–Queisser limit for single junction solar cells. Sol. Energy. **130**: 139–147.
23. Dargys A. and Kundrotas J. Handbook on physical properties of Ge, Si, GaAs and InP. Vilnius: Science and Encyclopedia Publishers, 1994.
24. Adachi S, 1989. Optical dispersion relations for GaP, GaAs, GaSb, InP, InAs, InSb, $Al_xGa_{1-x}As$, and $In_{1-x}Ga_xAs_yP_{1-y}$. J. Appl. Phys. **66**: 6030–6040.
25. Green M A, 2008. Self-consistent optical parameters of intrinsic silicon at 300 K including temperature coefficients. Sol. Energy Mater. Sol. Cells. **92**: 1305–1310.
26. Gradauskas J, Ašmontas S, Sužiedėlis A, Šilėnas A, Vaičikauskas V, Čerškus A, Širmulis E, Žalys O, and Masalskyi O, 2020. Influence of hot carrier and thermal components on photovoltage formation across the p-n junction. Appl. Sci. **10**: 1–8.
27. Sasaki M, Negishi H and Inoue M, 1986. Pulsed laser-induced transient thermoelectric effects in silicon crystals. J. Appl. Phys. **59**: 796–802.
28. Jayaraman S and Lee C H, 1972. Observation of two-photon conductivity in GaAs with nanosecond and picosecond light pulses. Appl. Phys. Lett. **20**: 392–395.

Masalskyi O. and Gradauskas J. 2022 Pre-themalizational effect of hot carriers on photovoltage formation in a solar cell. Ukr.J.Phys.Opt. **23**: 117 – 125. doi: 10.3116/16091833/23/3/117/2022

Анотація. *Практично досягнута ефективність перетворення енергії однопереходного сонячного елемента все ще значно нижча від теоретичної межі Шоклі-Квайссера і зростає дуже повільно з наступними роками. Ми вводимо явище гарячих носіїв як додатковий фундаментальний механізм власних втрат, який, як передбачається, відповідає за практичну недосяжність теоретичної межі ефективності. Всі сонячні фотони, крім тих, енергія яких дорівнює ширині забороненої зони напівпровідника, беруть участь у нагріванні носіїв і забезпечують цей процес більш ніж 52% всієї сонячної енергії.*

Ми також показуємо експериментальні доводи фотонапруги (ФН) гарячих носіїв у елементах з Si та GaAs яка зростає ще до процесу термалізації. Ця ФН протидіє класичній фотонапрузі, викликаній генерацією носіїв, та таким чином наноситься безпосередня втрата ефективності сонячного елемента з p-n переходом.